

KCL-PAKKA: Simulation of the 3D structure of paper

Kaarlo Niskanen¹, Niko Nilsen¹, Erkki Hellen² and Mikko Alava²

¹KCL Paper Science Centre, Box 70, 02151 Espoo, Finland
and

²Laboratory of Physics, Helsinki University of Technology, 02150 Espoo,
Finland

ABSTRACT

We present a novel approach to study the three-dimensional network structure of paper. In the KCL-PAKKA simulation model, the porous sheet structure is compiled from the different papermaking raw materials, fibres, fillers and fines. The model geometry is simplified in order to enable effective numerical experiments with arbitrary composition and layering. The KCL-PAKKA model gives realistic predictions for many paper properties. In this paper we describe the cross-over that occurs with increasing grammage from a thin strictly two-dimensional network to a thick layered networks. According to our simulations the cross-over occurs at low grammages, around 20 - 30 g/m², for papers made of stiff fibres (e.g. mechanical pulp) and at higher grammages, 40 - 80 g/m², for flexible fibres (e.g. beaten kraft). We discuss the statistical properties of the three-dimensional but layered random fibre network, particularly the bonding degree and pore geometry. In thick networks the pore geometry is isomorphic and only the length scale of the pores depends on fibre properties.

INTRODUCTION

The statistical geometry of two-dimensional random fibre networks is well-known from the work of Corte and Kallmes (1,2). Many features can be calculated exactly and others have been determined numerically (3). The two-dimensional approximation describes paper at low basis weights when all fibres that cross also bond to one another.

At normal basis weights paper contains pores between fibres that are not included in the analysis of Corte and Kallmes. Some attempts have been made to extend the analytical theory to real paper. In the "multiplanar model" the sheet is assumed to consist of a few layers each of which obeys the two-dimensional statistical network geometry (4). Recently this model has been developed further to describe the effects of fibre flexibility on paper density (5-7). The multiplanar model is not rigorous in the same sense as the Corte-Kallmes theory.

The structure of real paper is complicated, not only because of the random, intertwined and porous geometry, but also because of the many different constituents that paper is made of. Each furnish component contains fibres of different sizes as well as fibre fragments and fines. In practice paper properties are optimized by mixing together different furnishes. The structure of such a system cannot be readily described by analytical models.

We describe here a numerical simulation model that has been developed to study the structure of paper (8). The model allows us to combine different furnishes and fillers into a random fibre network with a porous planar structure very similar to that of real paper. From the generated structure we can predict all paper properties that are simply related to the network geometry. Perhaps the most notable exception are the mechanical properties whose dependence on the network geometry is still uncertain.

In this paper we concentrate on the statistical properties of the three-dimensional model network. The bonding degree and pore geometry are discussed in detail. The results are useful in understanding how the planar network structure of real paper differs from a two-dimensional system. Examples of practical applications of the KCL-PAKKA model are given in the Appendix.

KCL-PAKKA MODEL

It would consume a lot of computing time to calculate the precise three-dimensional geometry of the fibre network of paper. We have therefore simplified the problem as much as possible while keeping the essential physical features of the fibres, such as their dimensions and stiffness (8). Using the KCL-PAKKA model it is possible to generate realistic paper sheets in less than 10 minutes on an ordinary work station. The simulation program requires 10 - 20 Mb work space depending on various options.

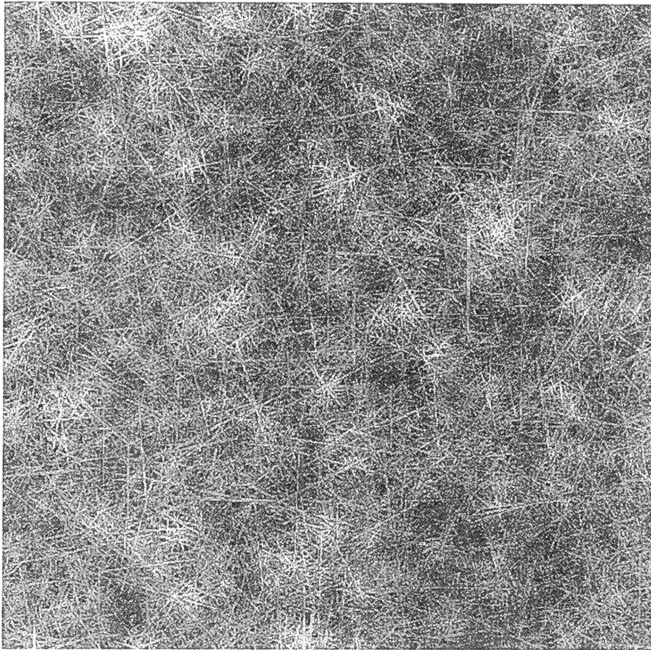


Figure 1: Illustration of the surface topography of a 45 g/m^2 (newspaper) sheet generated by the KCL-PAKKA model. Sheet size is $(0.7\text{cm})^2$.

In the simulations, straight fibres are deposited on a square lattice one by one, as if they were sedimenting from a dilute suspension with no inter-fibre correlations. The fibres are placed and oriented on the lattice at random (Fig. 1). Periodic boundary conditions are applied to fibres that cross the boundaries. The lattice is divided into square cells whose side length is $10\ \mu\text{m}$. This is the in-plane resolution of the model. Usually the substrate lattice consists of 1000×1000 cells so that the size of the model paper sheet is $1\ \text{cm}^2$. Sometimes smaller systems with fewer cells are used. The length l_f and width w_f of individual fibres are integer multiples of the unit length $10\ \mu\text{m}$. An arbitrary average fibre width can be generated with the alternate use of two unit widths.

We want the local coverage c (number of fibres covering the cell) always to be an integer. Therefore the fibres are deformed locally by small lateral displacements. The number of cells that a given fibre covers is fixed by the width and length of the fibre. Hence the end-to-end distance of fibres oriented along the lattice diagonal is $\sqrt{2}$ times the nominal fibre length. One can demonstrate (8) that normal fibre lengths $l_f \gg w_f$ have no effect on the sheet structure and thus the diagonal fibres induce only small errors to the geometric properties of the sheet. In spite of the simplifications the grammage and thickness distributions in the model sheets are quite realistic as Fig. 1 shows.

The non-trivial planar porous structure of real paper arises from the non-zero bending stiffness of the fibres. In the KCL-PAKKA model a bending flexibility T_f is defined through a constraint on the height of "steps" that the fibres can form:

$$|z_i - z_j| / t_f \leq T_f \quad (1)$$

where t_f is the fibre thickness and z_i and z_j are the elevations of the top surface of the fibre at any two nearest neighbor cells i and j that the fibre covers (Fig. 2). High values of T_f give dense and well-bonded sheets, while low values of T_f lead to bulky and porous sheets. The substrate lattice is flat. When new fibres land on it they are deformed in the z -direction to lie as low as possible while still obeying Eq (1). The vertical coordinates z_i are treated continuous variables.

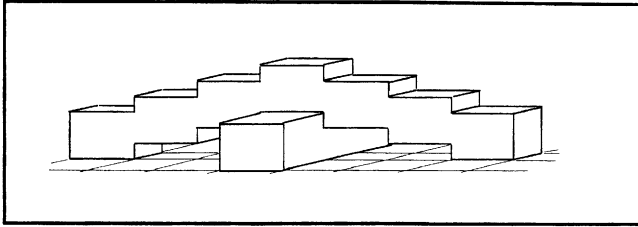


Figure 2: The bending mechanism of fibres in the model. The height of the "steps" (see text) is $T_f = 1/3$. Fibre width w_f is equal to the lattice unit.

The flexibility T_f can be related to the wet fibre flexibility WFF (9) through

$$T_f = (C w_f WFF)^{1/4} \quad (2)$$

where the constant $C = 5.4 \times 10^{-8}$ Nm depends in principle on the wet pressing pressure. We have fixed the value of C somewhat arbitrarily so that the simulated sheets roughly match handsheets in the physical properties. Experience has shown that it is impractical to use measured WFF -values directly in the simulations. Among other things, the WFF -values are usually not known for different fibre fractions. However, measured WFF -values serve as an indicator of relative differences between furnishes.

If one has only one type of fibres in the sheet, one can argue that the sheet structure should depend only on a dimensionless flexibility number (8)

$$F = T_f w_f / t_f \quad (3)$$

This is demonstrated in Fig. 3. The argument is based on the fact that fibre length has only a minor effect on the sheet structure. Then it is enough to consider fibre crossings. If F is held constant, changes in fibre properties affect only the lateral and vertical length scales of the network but they do not affect at all the fibre-to-fibre connections. Of course, the thickness and pore heights of the sheet are proportional to t_f . It may be of interest that the measured values of WFF (10) and known dimensions of paper-making fibres yield $F = 0.5 - 3$ while in actual simulations we have used somewhat higher values to reproduce measured paper properties (cf. Appendix).

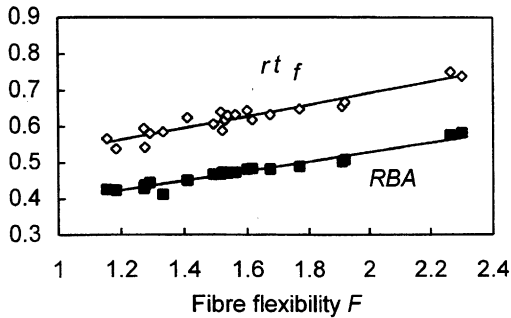


Figure 3: Relative bonded area (solid squares) and density (ρt_f , open diamonds) against fibre flexibility F . Fibre length l_f , width w_f , thickness t_f and WFF have been varied by $\pm 20\%$.

In addition to the flexibility, dimensions (length, width, thickness) and coarseness, certain optical values, such as the refractive index are also given to the fibres. Papermaking pulps are modelled with three or four fibre fractions, rather than with continuous distributions of the fibre dimensions. Typical fractions are the long fibres, two middle fractions and the fines. Fines and fillers are described according to the same principles as the fibres. Fines and fillers are inserted in groups that cover the unit. This is wrong locally but still correct in terms of the average structure.

The KCL-PAKKA model ignores many effects present in the real paper-making process. These include flocculation of fibres and hydrodynamic smoothing. The underlying sheet structure does not change when new fibres are deposited. The local interactions are replaced by an average force accounted for by T_r . At the same time the simple bending rule does not describe accurately even the effects of a hydrostatic pressure (11). Because the fibres deposit on a flat substrate lattice, the bottom side of the sheet becomes very smooth, much like a yankeedried paper surface. The top side resembles free-dried paper (12,13). It is also possible to mimic the calendering of the model sheets and thus obtain realistic surface roughnesses. Despite all its simplifications the model produces realistic paper properties. A few examples are given in the Appendix.

EVOLUTION OF PAPER STRUCTURE WITH INCREASING GRAMMAGE

The network structure of paper changes with grammage. At low grammages the network is two-dimensional with no inter-fibre pore space in the thickness direction. At higher grammages inter-fibre pores appear in the z -direction and lead to non-trivial sheet properties. In the following we discuss (14) the basic network geometry using the KCL-PAKKA model with just one type of fibres. The network properties are characterized by three numbers, the average coverage \underline{c} , relative bonded area RBA and the average pore number \underline{p} . Density ρ is briefly considered in the end of this section.

The fibre properties are characterized by the dimensionless flexibility F . The fibre length $l_f \gg w_f, t_f$ does not affect the network properties (8). Unless otherwise indicated, in the following all fibres are confined to lie along the two lattice axes (14). The orthotropic orientation in place of isotropic orientation causes certain irregularities in the results when F is an integer.

Coverage \underline{c} is the average number of fibres covering a cell. In reality the grammage of a single fibre is 5 - 10 g/m² so that ordinary paper corresponds to $\underline{c} = 5 - 20$. Coverage is a precise measure of the number of fibre layers in a sheet, unlike other measures based on the average thickness of a fibre layer. Pore number \underline{p} is the average number of pores per unit cell. The relative bonded area RBA gives the connectivity of the network, the frequency of bonded fibre surface. Only the in-plane fibre surfaces are considered here. Thus RBA is defined as the average contact area of a fibre divided by the total area $2l_f w_f$. The porous structure and the free surfaces imply $RBA \leq 1$.

Consider first the special case where the fibres are either infinitely flexible or infinitely thin so that $F = \infty$. The network is then two-dimensional. The only "pores" are vacancies, cells covered with no fibres. Poisson statistics implies that the number of vacancies \underline{v} and RBA are given by

$$\underline{v} = \exp(-\underline{c}) \quad (3)$$

and

$$RBA = 1 - [1 - \exp(-\underline{c})] / \underline{c} \quad (4)$$

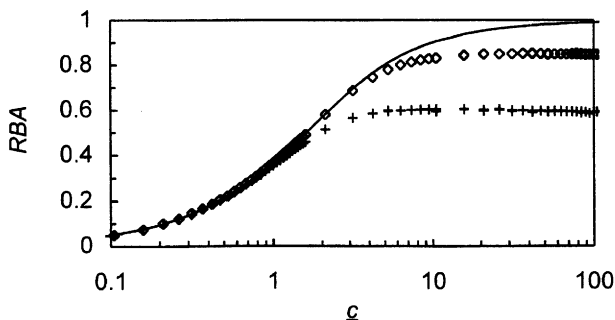


Figure 4: RBA against coverage \underline{c} for $F = 1$ (crosses) and 2 (diamonds) (8). Solid line gives the exact solution for $F = \infty$, Eq. (4).

The simulation model with both orthotropic xy -orientation and the isotropic orientation agrees with Eq. (4) when $F = \infty$. When the fibres have a finite flexibility and non-zero thickness, pores occur between the fibres in the z -direction when coverage increases. The RBA still increases with coverage as Eq. (4) predicts, but only at low \underline{c} (Fig. 4). At higher coverages RBA has a weak maximum, and then becomes constant*, $RBA \rightarrow RBA_{\infty}$. The maximum arises because \underline{p} increases with coverage (see below) and counteracts the decrease in \underline{v} . It is easy to see that the proper generalization of Eq. (4) is

$$RBA = 1 - [1 - \exp(-\underline{c})] [\underline{p} + 1] / \underline{c} \quad (5)$$

In real paper sheets the maximum may be absent because of the smoothing wet pressing action, or it may be enhanced because hydrodynamic resistance to sheet compaction increases with grammage.

At high coverages every new "layer" of fibres has the same structure as the preceding one. The pore number increases linearly with coverage (Fig. 5):

$$\underline{p} = p'_{\infty} \times (\underline{c} - c_0) \quad (6)$$

* The subscript " ∞ " is used for values in the high-coverage bulk region

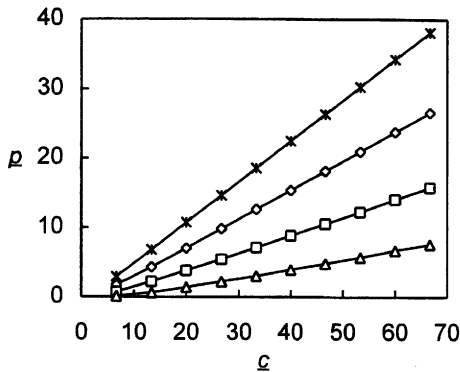


Figure 5: Pore number ρ against coverage c for $F = 0.5$ (crosses), 1.1 (diamonds), 2.1 (squares) and 4.1 (triangles).

The coverage c_0 measures the statistical cross-over from a two-dimensional system to a three-dimensional bulk phase (see also Fig. 4). At $c > c_0$ three-dimensional pores develop in the network, as opposed to the two-dimensional vacancies at low c .

When the fibre flexibility increases, there are fewer pores in the network and the cross-over coverage c_0 is larger. Orthotropic geometry with one type of fibres causes the non-monotonic oscillations in Fig 6(a). They would disappear if isotropic orientation or distributed F were used. In that case c_0 is roughly given by

$$c_0 \approx 1 + 2F \quad (7)$$

Observe that no pores exist at $c < 1$ and hence necessarily $c_0 \geq 1$ for all F . From the comparison of KCL-PAKKA simulations with real paper properties we can conclude that $F \approx 1$ for stiff mechanical fibres and $F = 3-4$ for flexible beaten kraft fibres. These values correspond to $c_0 = 3$ and 7-8, respectively, for the cross-over coverage or 20-30 g/m^2 and 40-80 g/m^2 for paper grammage.

In the three-dimensional bulk phase ($\underline{c} > c_0$) $p'_\infty = 1 - RBA_\infty$. The expression

$$p'_\infty = 1 - RBA_\infty \cong [1 - \exp(-2F)] / 2F \tag{8}$$

similar to Eq. (4) at the two-dimensional limit, gives surprisingly good a match to the simulated data (Fig. 6(b)). Equation (8) gives the maximum bonding degree that is achievable for a given F .

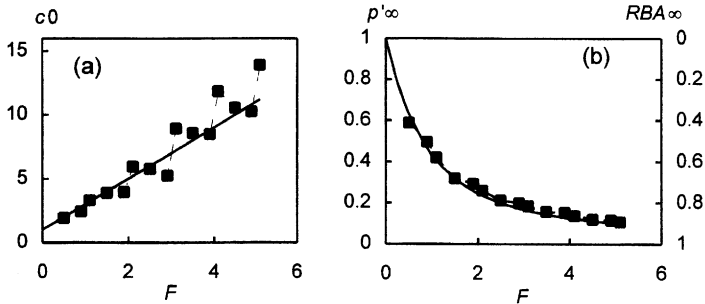


Figure 6: The cross-over coverage c_0 (a) and slope p'_∞ (b) against the dimensionless fibre flexibility F . Eqs. (7) and (8) correspond to the solid lines in a and b, respectively.

Now consider the network density. Its evaluation is complicated by the rough surfaces of the network. The effective density ρ can be defined as the volume fraction of the sheet that is occupied by the fibres. Hence $\rho \leq 1$. The apparent density that one measures in practice is a lower bound for ρ . The apparent density can also be evaluated in the simulations if an assumption is made about surface compression in the measurement. We have assumed that the compression is such that 10% of the top surface of the sheet makes contact with the flat head of the thickness meter.

When coverage increases, the effective density ρ decreases monotonically as more pores develop (Fig. 7). There is no simple relation between RBA and ρ when \underline{c} varies. On the other hand, at any fixed coverage RBA and ρ are ap-

proximately in a linear relationship when fibre properties (as given by F) vary. The relationship also depends on the fibre orientation distribution. The linearity holds particularly well if the orthotropic xy -orientation is used in the simulations (8) but not quite as well with the more realistic isotropic orientation. The latter case is plotted in Fig. 8. Assuming that fibre grammage is 5 g/m^2 , the three coverages plotted, $\underline{c} = 5, 10$ and 20 , correspond to paper grammages $25, 50$ and 100 g/m^2 .

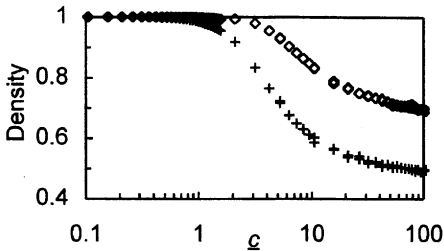


Figure 7: Effective density ρ against coverage \underline{c} for $F = 1$ (crosses) and 2 (diamonds); same systems as in Fig 4.

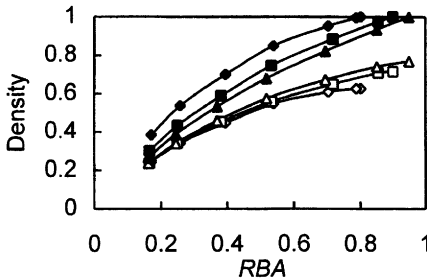


Figure 8: Effective density (closed symbols) and apparent density (open symbols) against RBA for $\underline{c} = 5, 10$ and 20 (diamonds, squares and triangles, respectively). The symbols are located roughly at $F = 0.5, 1, 2, 4$ etc. Isotropic fibre orientation.

The higher is the coverage, the lower is the effective density for a fixed *RBA* or fixed fibre flexibility *F*. The simulated apparent density behaves in the opposite manner and is much less sensitive to coverage. Notice that when *F* increases, the *RBA* is bounded from above by Eq (4). When *F* decreases towards zero, the model becomes unrealistically sparse since tilting of the fibres is not allowed. The simulation values in that end are also dependent on the fibre length through w_f/l_f . The results in Fig. 8 are calculated for $l_f = 3$ mm and $w_f = 40$ μ m.

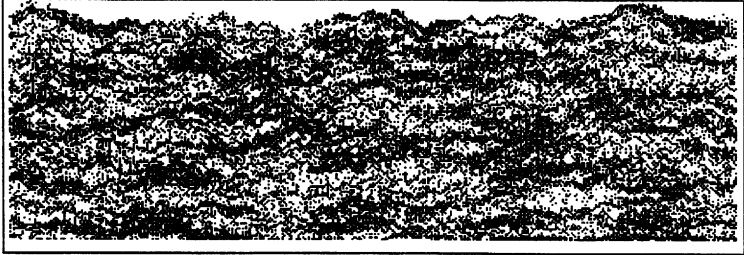


Figure 9: Illustration of the porous network geometry at a high coverage $\varrho = 83$. Fibres are given in black and pores in white.

PORE SIZE DISTRIBUTIONS

Figure 9 illustrates the porous cross-section geometry generated in the KCL-PAKKA model. In the following we show how the distribution of pore sizes change as the fibre flexibility is changed. The pores in our model are defined as vertical openings between fibres. The open space between the network and the flat substrate lattice is not considered as pores. Cavities, i.e. cells of zero local coverage are also excluded from the analysis.

We limit the analysis to pore heights h , i.e. the vertical distances between fibres. The height of pores is evaluated separately for every cell so that the pore height distribution $G(h)$ goes through all the cells and all the pores above every cell. This definition instead of using some sort of average height of a pore avoids all

the ambiguities that would arise if one had to define what a pore really is. The same pore height distribution can also be evaluated from cross sections of real paper sheets. Figure 10 shows that the simulated pore height distribution $G(h)$ is exponential except for small deviations at low h (14). The orthotropic xy-orientation and fibres with constant F are used here but the exponential dependence also holds with isotropic orientation. The unrealistically high bins of t_r are used here to average out unphysical fluctuations from $G(h)$. Such fluctuations are absent with distributed F or isotropic fibre orientation.

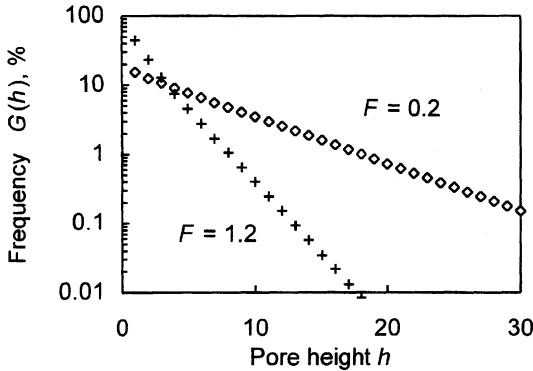


Figure 10: Pore height distribution $G(h)$ for $F = 0.2$ and 1.2 (diamonds and crosses, respectively) at a high coverage $\varrho = 83$. Pore heights h are rounded up to the nearest integer multiple of t_r . Orthotropic xy-orientation distribution. Vertical scale is logarithmic.

If the exponential pore height distribution is defined as

$$G(h) \approx (1/h_0) \exp(-h/h_0) \quad (9)$$

then simulation results (14) with orthotropic fibre orientation suggest that at high coverages, in the three-dimensional bulk phase

$$h_0 \approx t_r / RBA_\infty \quad (10)$$

Even though the result only applies to high coverages and one single fibre type, it suggests that there *maybe* a simple relationship between the distribution of pore heights and the *RBA* of real paper, too.

As already pointed out, the shape and size of pores in paper cannot be defined unambiguously. The pores are connected through a network of narrow “throats” and measurements of the pore size distributions are related to the cross-sectional areas of these throats. Therefore it would be difficult to define pores in the simulations in such a way that their size distribution could be directly compared with measurements.

Elsewhere (14) we have briefly considered various definitions for the in-plane area of pores. The relatively small size of the simulation system limits the statistics more than it does for the pore heights. However, it seems that also the distribution of pore areas is roughly exponential and insensitive to the definition of the pore area. Furthermore, at high coverages the average area of pores $\langle A \rangle$ is inversely proportional to *RBA*,

$$\langle A \rangle \approx t_f^2 / RBA_\infty \quad (12)$$

We conclude that the pore size distribution in paper seems to be isomorphic, independent of fibre properties. The distribution of the pore height and area are roughly exponential and fibre properties affect only the length scales of the pores (i.e. $\langle h \rangle$ and $\langle A \rangle$).

CONCLUSIONS

We have used the numerical KCL-PAKKA model to study the three-dimensional structure of paper when coverage and fibre flexibility vary. The effects of fibre flexibility are described by the dimensionless parameter *F*.

At low grammages the network is two-dimensional. With increasing coverage, above the critical coverage $c_0 \approx 1 + 2F$, a bulk phase develops. According to the simulations the cross-over coverage corresponds to 20-30 g/m² and 40-80 g/m² in paper grammage for stiff mechanical fibres and flexible beaten kraft fibres, respectively. Hence papers made of mechanical furnish could usually be charac-

terized as three-dimensional layered networks whereas the properties of papers made of kraft pulp would still be intermediate between two-dimensional and three dimensional networks.

The three-dimensional bulk phase is isomorphic in structure, qualitatively independent of fibre properties. The pore sizes (height and in-plane area) are roughly exponential with the decay rate inversely proportional to RBA which in turn is a monotonically increasing function of F . The frequency and size of pores decrease when F increases.

ACKNOWLEDGMENTS

This study was financially supported by the Technology Development Centre of Finland and the Academy of Finland which is gratefully acknowledged.

REFERENCES

1. Corte H, Kallmes OJ, "Statistical geometry of a fibrous network", in Formation and Structure of Paper, (edited by F Bolam), British Paper and Board Makers Assoc., London, 13-46 (1962).
2. Corte H, Kallmes OJ, "The structure of paper. I The statistical geometry of ideal two dimensional fiber networks", Tappi J. 43(9):737-752 (1960).
3. see e.g. Deng M, Dodson CTJ, "Paper as an engineered stochastic structure", Tappi Press, Atlanta (1994), Chapters 3 and 5.
4. Kallmes O, Corte H, Bernier G, "The structure of paper. II The statistical geometry of multi-planar fibre network", Tappi J. 44(7):519-528 (1961).
5. Görres J, Sinclair CS, Tallentire, A, "An interactive multi-planar model of paper structure", Paperi ja Puu 71(1):54-59 (1989).
6. Gorres J, Luner P, "An apparent density model of paper", J. Pulp Paper Sci. 18(4):J127-130 (1992).

7. Gorres J, Amiri R, Wood JR, Karnis A, "The apparent density of sheets made from pulp blends", *Tappi J.* 79(1):179-187 (1996); and references therein.
8. Niskanen KJ, Alava MJ, "Planar random fibre networks with flexible fibres", *Phys. Rev. Lett.* 73(25): 3475-78 (1994).
9. Steadman R, Luner P, "The effect of wet fibre flexibility on sheet apparent density", in *Papermaking raw materials* (edited by V Punton), Mechanical Engineering Publ. Ltd., London, 311-338 (1985).
10. Paavilainen L, "Conformability - flexibility and collapsability - of sulphate pulp fibres", *Paperi ja Puu* 75(9-10):689-702 (1993).
11. Sherwood JD, Van Damme H, "Nonlinear compaction of an assembly of highly deformable platelike particles", *Phys. Rev.* E50(5): 3834-3840 (1994).
12. Seppälä E, Alava M, Niskanen K, "Can the effect of furnish be detected in the roughness of handsheets?" (in Finnish), *Paperi ja Puu* 78(8):446-449 (1996).
13. Mangin PJ, Béland M-C, Cormier LM, "A Structural Approach to Paper Surface Compressibility -- Relationship with Printing Characteristics", in *Products of Papermaking* (edited by CF Baker), PIRA International, Vol. III, 1397-1425 (1993).
14. Hellén E, Alava MJ, Niskanen KJ, "Porous Structure of Thick Fibre Webs", to be published in *J Appl. Phys* (1997).

APPENDIX: SAMPLE RESULTS FROM KCL-PAKKA SIMULATIONS

KCL-PAKKA		v6.0								
Copyright Oy Keskuslaboratio 1995										
Newsprint, TMP, CSF 100				Homogeneous isotropic sheet				No calendering		
Mass	Fibre dimensions			flexibility		refractive index		coarseness		
fractions	length (m)	width (um)	thickn (um)	Tf	F	n	n'	(mg/m)		
0.39	2.7	42	11	0.26	0.99	1.55	80	0.370		
0.21	1.7	34	8.5	0.27	1.09	1.55	90	0.231		
0.15	0.6	28	6.3	0.30	1.32	1.55	90	0.141		
0.25	0.03	30	1	30.05		1.55	100	0.024		
grammage	density	apparent density	bulk	thickness	light scattering	light absorption	opacity	R_0	Y-value	
g/m2	kg/m3	kg/m3	cm3/g	um	m2/kg	m2/kg	%	%	%	
30	571.1	365.8	2.734	82	53.18	2.39	78.4	58.13	74.14	
33	555.5	366.1	2.732	90.2	53.41	2.38	80.89	60.05	74.24	
36	541.4	365.8	2.734	98.4	53.75	2.39	83.14	61.75	74.28	
39	528.7	365.2	2.739	106.8	53.96	2.39	85.05	63.21	74.32	
42	518.6	365.8	2.734	114.8	54	2.38	86.66	64.44	74.35	
45	509.1	365.7	2.735	123.1	54.21	2.4	88.18	65.56	74.35	
48	500.7	365.4	2.737	131.4	54.3	2.39	89.42	66.53	74.4	
51	493.2	365.7	2.735	139.5	54.16	2.38	90.46	67.33	74.42	
54	486.9	366	2.733	147.6	54.41	2.39	91.52	68.12	74.43	
57	480.8	366.2	2.731	155.7	54.5	2.39	92.41	68.8	74.45	
60	475.3	366.3	2.73	163.8	54.66	2.38	93.17	69.43	74.52	
error estim	1.1	1.7	0.013	0.8	0.58	0.05	0.2	0.11	0.14	
grammage	bending stiffness	elastic modulus	tensile index	tensile strength	bonded area	RBA of fibre fractions				
g/m2	mNm	MPa	Nm/g	N/m	m2/kg	weighted average	fraction 1	fraction 2	fraction 3	
30	0.023	1910	41.19	1236	199.4	0.394	0.391	0.401	0.408	
33	0.033	1912	41.18	1359	199.3	0.395	0.393	0.4	0.407	
36	0.047	1910	41.18	1483	199.3	0.395	0.392	0.399	0.408	
39	0.064	1906	41.18	1606	199.3	0.394	0.391	0.399	0.408	
42	0.085	1910	41.17	1729	199.2	0.394	0.391	0.399	0.408	
45	0.11	1909	41.16	1852	199.2	0.393	0.39	0.399	0.407	
48	0.14	1907	41.14	1975	199.1	0.392	0.389	0.399	0.406	
51	0.176	1908	41.13	2098	199	0.392	0.388	0.399	0.406	
54	0.217	1909	41.12	2220	199	0.392	0.389	0.397	0.405	
57	0.265	1909	41.10	2343	198.9	0.391	0.389	0.396	0.405	
60	0.32	1909	41.09	2465	198.8	0.391	0.388	0.396	0.404	
error estim	0.001	8	0.02	1	0.1	0.001	0.002	0.001	0.002	

KCL-PAKKA		v6.0							
Copyright		Oy Keskuslaboratorio 1995		Three-ply isotropic sheet					
Folding box board				SWK, CSF 360		No calendring			
				HWK, SR 23					
Three-ply structure:		40 + 100 + 40 g/sqm		Bl. GW					
Coating		10 g/sqm both sides							
Mass		Fibre dimensions		flexibility		refractive index		coarseness	
fractions	length (m)	width (um)	thickn (um)	Tf	F	n	n'	(mg/m)	
Middle layer									
0.027	3.4	40	6.6	0.683	4.14	1.55	4	0.29 SWK	
0.014	2.1	30	4.4	0.737	5.03	1.55	5	0.145	
0.009	1.2	24	2.4	0.803	8.03	1.55	5	0.063	
0.006	0.03	30	0.7	30.053		1.55	5	0.023 fines	
0.016	1.8	35	5.9	0.66	3.92	1.55	8	0.206 HWK	
0.066	1.2	29	5.2	0.697	3.89	1.55	8	0.151	
0.067	0.6	24	3.8	0.713	4.50	1.55	8	0.091	
0.017	0.03	30	0.7	30.053		1.55	8	0.021 fines	
0.084	1.9	39	11.6	0.257	0.86	1.55	19	0.396 Bl. GW	
0.081	1	36	10.2	0.25	0.88	1.55	19	0.321	
0.1	0.5	32	9	0.243	0.86	1.55	19	0.252	
0.07	0.05	30	1	30.053		1.55	20	0.026 fines	
Surface layers									
0.043	3.4	40	6.6	0.683	4.14	1.55	4	0.29 SWK	
0.02	2.1	30	4.4	0.737	5.03	1.55	5	0.145	
0.014	1.2	24	2.4	0.803	8.03	1.55	5	0.063	
0.009	0.03	30	0.7	30.053		1.55	5	0.023 fines	
0.035	1.8	35	5.9	0.66	3.92	1.55	8	0.206 HWK	
0.145	1.2	29	5.2	0.697	3.89	1.55	8	0.151	
0.143	0.6	24	3.8	0.713	4.50	1.55	8	0.091	
0.035	0.03	30	0.7	30.053		1.55	8	0.021 fines	
grammage	density	apparent density	bulk	thickness	light scattering	light absorption	opacity	R ₀	Y-value
g/m2	kg/m3	kg/m3	cm3/g	um	m2/kg	m2/kg	%	%	%
200.4	582.3	514.1	1.945	351	42.62	0.37	97.39	85.3	87.59
grammage	bending stiffness	elastic modulus	tensile index	tensile strength	bonded area	RBA weighted average			
g/m2	mNm	MPa	Nm/g	N/m	m2/kg				
200.4	2.226	2666	51.3	9255	198.5	0.668			
grammage	RBA of middle ply			HWK fibre fractions			Bl. GW fibre fractions		
g/m2	fraction 1	fraction 2	fraction 3	fraction 1	fraction 2	fraction 3	fraction 1	fraction 2	fraction 3
200.4	0.602	0.608	0.612	0.603	0.612	0.613	0.546	0.544	0.546
grammage	RBA of surface ply			HWK fibre fractions					
g/m2	fraction 1	fraction 2	fraction 3	fraction 1	fraction 2	fraction 3			
200.4	0.757	0.78	0.779	0.757	0.774	0.776			

Transcription of Discussion

KCL-PAKKA: Simulation of the 3D structure of paper

Kaarlo Niskanen, KCL, Finland

Jim Luce, Paper Performance, USA

Thank you Dr Niskanen. I think the introduction of fibre flexibility is a major step in making the properties of these virtual papers more closely resemble that of real papers. My question is, do you believe it would be useful, or for that matter even possible, to modify the base plane of your virtual sheet former to represent the topography of a forming fabric?

Kaarlo Niskanen

Yes, it is definitely possible. Of course the structure we have is 1cm a side so you only reproduce substrate that has a structure below that length scale but basically it is quite possible. Perhaps I should also say that this structure we are generating obviously is two-sided because on one side the fibres land on a flat surface and the other side is like a mountain landscape. We are working on a system to provide a symmetrical structure when you have calendering effects and so on. The weave marking is not the first thing we look at.

John F Waterhouse, Senior Associate Scientist, IPST, USA

I think it is a very nice model that you've created but in a 1985 review paper published in a book by STFI I showed there that for four pulps, using the data of Renel, that there was a very good correlation between RBA and density, and the densification was produced by changing wet pressing and refining. I'm just looking at your Figure 8 where you've got an envelope, but it would seem to me that in terms of 'F' you perhaps could account for beating and wet pressing - I'm not quite sure how but may be you've thought about that - however there isn't an envelope for a specific pulp, but there is a very good correlation between RBA and density. The other quick comment is this. It seems that in your model, and again we have published data on this², that there is a change in average pore size at a fixed density when you look at refining and wet pressing. It seems that this should be a part of your model.

¹ Design Criteria for Paper Performance, Ed. P Kolseth, C Fellers, L Salmen, and M Rigdahl, STFI-Meddelande A 969, August 1987

² Bitler, T and Waterhouse, TAPPI J 76(9): September 1993

Kaarlo Niskanen

On the latter point I completely agree with you that it should come out and we think we know more or less how beating affects this sort of flexibility as it's modelled in the simulation system that we've got. The other part about density and relative bonded area I, for one, firmly believe that it's quite useful to use density as a measure of relative bonded area, but to my disappointment there is no simple equation that you could use there that would say how the relationship actually goes. You can do a linear regression and that works fine but there is no beautiful mathematics behind it, or simple formulation.

Derek Page

I wonder if you could clarify for me what you've done because I'm still confused. Your Figure 1 shows what appears to me to be a 2 dimensionally random structure, that is, all orientations. Your Figure 2 doesn't show all orientations, it shows simply fibres at right angles to one another. Which is your PAKKA model - a model where the fibres are at right angles to one another or a model where they are 2 dimensionally randomly orientated?

Kaarlo Niskanen

We can do both. It was just easier to draw that way.

Derek Page

But your calculations are done on what? Which model?

Kaarlo Niskanen

Yes, that's a bit confusing. Most of them are done on an orthotropic, rectangular system but some others like this RBA-density graph is done for isotropic distribution. I think it's clear at each point in the text which one we've used. The RBA density figure, Figure 8, that Prof Waterhouse referred to. That is done for isotropic, completely random distribution.

Derek Page

Just one other point, RBA and density. Are you assuming that when two fibres cross one another that they are in contact over that whole area?

Kaarlo Niskanen

Yes of course. I'm assuming it, I'm not saying it happens in reality.

Derek Page

I would be very wary about using your values of RBA and comparing them with RBAs from any measurement that we normally use including taking cross-sections or more specifically taking scattering coefficients because the crossing area isn't generally completely bonded. It's a function of beating time, and it's a function of pressing pressure. For very lightly bonded sheets you may only get about 10-20% of that crossing area which is actually in bonded contact so I just wanted to warn people not to try, and John Waterhouse particularly, not to use this estimate of RBA and compare it with a measurement made by scattering coefficients.

Kaarlo Niskanen

If I may I'd like to say I completely agree and we just have a very specific definition for the relative bonded area, one could put in other types of geometry for fibre cross-sections, that's no problem.

Derek Page

Please don't redefine RBA, we know what we mean by RBA. If you want to give it another term do!

Kaarlo Niskane

n

Then it's a question of whether you want to look at the molecular level or optical level or what. What is your RBA anyway?

Professor Jacques Silvy, Universidade da Beira Interior, Portugal

A very interesting contribution to show the effect of the flexibility of the fibres on what we call the thesselation of particles in a structure. One point I think we must be aware of, is your definition of a 3 dimensional model. How could you say it is a 3 dimensional model if you restrict your analysis to only one direction? You take the isotropy as a matter of fact in your model but we know that the anisotropy in the plane has a big influence on the paper properties; for instance how could you predict the permeability of

the sheet if you only look at the thickness of the pore in the z-direction?

Kaarlo Niskanen

We have a complete 3 dimensional structure. We know the entire structure and we can put in any fibre orientation you wish. We can calculate any parameter you want us to calculate but those things get so messy. There are some things that are beautiful and nice and those are the ones that are presented here. On the question of permeability, even if we knew the geometry you can't calculate the permeability directly from the geometry.

Jacques Silvy

Yes we do. If we have the viscosity of the fluid and the pressure exerted, you could do it in any direction, but with a 3 dimensional model; it means that you need to explore the structure in every direction.

Kaarlo Niskanen

As I said we can explore the structure in any direction, but I only had half an hour. I can calculate whatever parameter you wish me to calculate. Ref K1 (published in J. Appl. Phys 81 (1997):9, 6425-6431) contains more information on the 3D structure. Even an analytic approximation is given for permeability but its reliability is most questionable.

Jose Iribarne, PhD Student, State University of New York, USA

Do you see any change in the distribution of pores across the thickness of the sheet or that will require a length distribution of the fibres?

Kaarlo Niskanen

There is, in this case, a rare distribution in the thickness direction because we are putting fibres on a flat surface. Basically if you think of this as a growth problem, this cross-over from non-porous to porous structure happens when the new fibres no longer feel the flat substrate. So there's definite profile in the pore volume in the thickness direction, but we haven't looked at that in detail.

Jose Iribarne

I'm glad we have a paper product that we can sell through the internet!!

Kaarlo Niskanen

If anyone buys it that's another thing!!

Tetsu Uesaka, Director, Paprican, Canada

In my understanding you have not yet considered the essential effect of wet pressing. Normally wet pressing introduces quite strong spatial correlation between height and mass density and so on. By simply saying higher mass density area tends to be compressed more, therefore the distribution of the pores and the correlation structure between mass density and the pore structure are altered. Are you considering this?

Kaarlo Niskanen

We have the average wet pressing pressure through this formula which gives us the effect of flexibility in the same way as it's done in the measurement of wet fibre flexibility (Steadman method). So that's taken in but the spatial correlations are not. We are working on that.